Proceedings of the International Association for
Shell and Spatial Structures (IASS) Symposium 2013
„BEYOND THE LIMITS OF MAN"
23-27 September, Wroclaw University of Technology, Poland
J.B. Obrębski and R. Tarczewski (eds.)

Interactive Form-Finding of Elastic Origami

Tomohiro Tachi

Assistant Professor, The University of Tokyo, Tokyo, Japan, *tachi@idea.c.u-tokyo.ac.jp*

Summary: In this paper, we propose a novel computational method to simulate and design origami whose form is governed by the equilibrium of forces from the elastic bending of each panel. In special, we explore statically indeterminate origami structure that can be manipulated by pin supporting finite number of vertices. The computational method is proposed so that we can interactively explore the design space of such origami form. The concept of kinematic origami tessellation based on bending of panels is introduced.

Keywords: *Origami, Morphology, Kinematics, Rigid Origami, Form-finding*

1. INTRODUCTION

The form of origami made of thin sheet material is governed by bending as well as rigid origami mechanism, i.e., panel and hinge mechanism. For example, some classes of quadrangle-based origami form one-DOF mechanism as rigid origami while such a structure can be flexibly bent and twisted when each quadrangle panel bends in the diagonal direction (Fig. 1). Here, the form is governed by the boundary conditions and equilibrium of stresses from the bending of each panel. This yields an interesting variety of forms with double curvatures potentially useful for the fabrication based on self-folding and bending and for transformable and flexible structures and architectural components for responsive environments. However, existing kinematic method for rigid origami simulation cannot be applied to appropriately capture such an elastic behavior of origami.

In this paper, we present a novel computational method for interactively simulating and designing origami whose form is governed by the bending of each panel. The bending of each panel is modeled by an angular spring between facets. The valid form is described by the equilibrium of the bending moment. Unlike a straightforward form-finding approach based on minimizing bending energy while fixing the support conditions, we introduce geometric constraints that keep the form to be under equilibrium. Our method naturally avoids impossible support conditions by handling support positions also as variables. We introduce an interactive form finding system of such elastic origami. We introduce the concept of an elastic origami tessellation that can be kinematically controlled by actuating the positions of the supporting vertices.

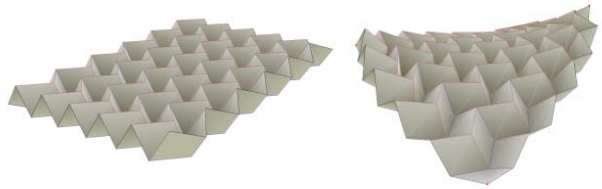

Fig. 1: Twisting Miura-ori.

2. BENDING

We first represent an origami surface as a triangular mesh rigid origami by triangulating non-triangular facets (quadrangles etc.) and also by adding sufficient number of foldlines representing the smooth bending behavior. This model can be represented as an unstable truss mechanism in which each edge is a rigid bar. Such a mechanism has $n_0 - 3$ degrees of freedom of transformation when n_0 is the number of edges on the boundary of the mesh, if the structure is a topological disk [1].

Then, the form is stabilized by the equilibrium of the force from the elastic bending of each panel which is represented by the angular springs at the edges added to triangulate panels. The angular moment $M_i(\rho_i)$ at edge i is given by the function of the folding angle ρ_i. The angular moments are first converted into equivalent forces applied at the nodes. Following the notation in Fig. 2, Angular moment M_{uv} at edge uv applied to triangle uvw is equivalently represented by the forces $\mathbf{f}_u$, $\mathbf{f}_v$, and $\mathbf{f}_w$ at vertices u, v, and w, respectively, as

$$\mathbf{f}_u^{uv} = -\frac{M_{uv}}{l_{uv}} \cot\theta_v \, \mathbf{n} \tag{1}$$

$$\mathbf{f}_v^{uv} = -\frac{M_{uv}}{l_{uv}} \cot\theta_u \, \mathbf{n} \tag{2}$$

$$\mathbf{f}_w^{uv} = \frac{M_{uv}}{h_w}\mathbf{n}, \tag{3}$$

where h_w is the height, and θ_u and θ_v are the base angles when edge uv is set as the base.

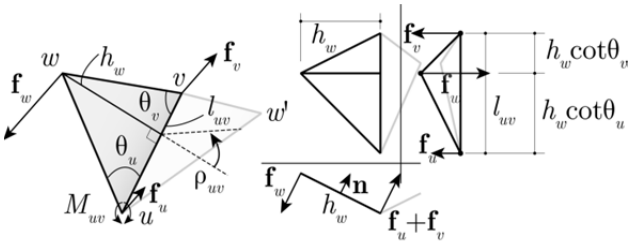

Fig. 2: Force applied to triangle *uvw*.

Here, we assume the constant stiffness angular spring as,

$$M_i(\rho_i) = -k_i \frac{l_i}{h_i}\rho_i, \tag{4}$$

where l_i is the length of the edge and h_i is the mean height. In this case, we use harmonic mean $\frac{1}{h_{uv}} = \frac{1}{2}\left(\frac{1}{h_w} + \frac{1}{h_{w'}}\right)$ when uvw and vuw' denote the incident two triangles.

Here, Equation (4) is chosen so that the angular moment is 1) proportional to the edge length when the height is constant and 2) scale independent when the shapes are similar. These properties are necessary because of the consistency with respect to 1) splitting and 2) scaling operations. 1) If edge of length l is split into arbitrary two portions with lengths l^1 and l^2 ($l^1 + l^2 = l$), the moment must satisfy $M(l^1) + M(l^2) = M(l)$ because otherwise the same geometric forms with different meshing can produce different angular moment. 2) The total bending energy of thin elastic shell E is given by $E \propto \frac{1}{2}\int \kappa(\mathbf{x})^2 dA$. If the bent form is scaled by factor s, then the curvature is given by $\kappa'(\mathbf{x}) = \kappa(\mathbf{x})/s$ and the area $A' = s^2 A$. Then, $E' = E$ and thus $M = \frac{\partial E}{\partial \rho}$ is scale independent (Fig. 3).

The forces are then written as

$$\mathbf{f}_u^{uv} = \frac{k_{uv}}{h_{uv}}\rho_{uv} \cot\theta_v \, \mathbf{n} \tag{5}$$

$$\mathbf{f}_v^{uv} = \frac{k_{uv}}{h_{uv}}\rho_{uv} \cot\theta_u \, \mathbf{n} \tag{6}$$

$$\mathbf{f}_w^{uv} = -\frac{k_{uv}}{h_{uv}}\rho_{uv}(\cot\theta_u + \cot\theta_v)\mathbf{n}, \tag{7}$$

The equilibrium of bending and axial forces is a necessary condition for the model to be in a valid configuration. Here, we use force densities $w_{uv} = f_{uv}/l_{uv}$ to represent the axial force f_{uv} at edge uv. Then, for each structurally unconstrained vertex u,

$$\mathbf{F}_u = \mathbf{B}_u + \mathbf{A}_u = \sum_{\substack{\text{edge } i \text{ adjacent} \\ \text{or incident to } u}} \mathbf{f}_u^i + \sum_{v \text{ incident } u} \mathrm{w}_{uv}(\mathbf{x}_v - \mathbf{x}_u) = \mathbf{0}. \quad (8)$$

For structurally constrained vertex u (pin supported), $-\mathbf{F}_u$ equals the reaction force from the support. The concept of force density originates in [2]; however, we allow force densities to vary unlike in the original force density method, in which $\mathbf{w}$ is constant. The configuration of the structure is represented by the vertex coordinates $\mathbf{x} = \{\mathbf{x}_1^{\mathrm{T}} \ \cdots \ \mathbf{x}_V^{\mathrm{T}}\}^{\mathrm{T}} = \{x_1 \ y_1 \ z_1 \cdots x_V \ y_V \ z_V\}^{\mathrm{T}}$ and the force densities $\mathbf{w} = \{w_1 \ \cdots \ w_{\mathrm{E}}\}^{\mathrm{T}}$ where the number of vertices is V and the number of edges is E. Vector equation $\mathbf{F}(\mathbf{x}, \mathbf{w}) = \{\mathbf{F}_1^{\mathrm{T}} \cdots \mathbf{F}_V^{\mathrm{T}}\}^{\mathrm{T}} = \mathbf{0}$ confines the configuration to a subspace within which infinitesimal variation $\begin{Bmatrix}\delta\mathbf{x}\\ \delta\mathbf{w}\end{Bmatrix}$ satisfies

$$\begin{bmatrix}\frac{\partial \mathbf{F}}{\partial \mathbf{x}} & \frac{\partial \mathbf{F}}{\partial \mathbf{w}}\end{bmatrix}\begin{Bmatrix}\delta\mathbf{x}\\ \delta\mathbf{w}\end{Bmatrix} = \mathbf{0}. \quad (9)$$

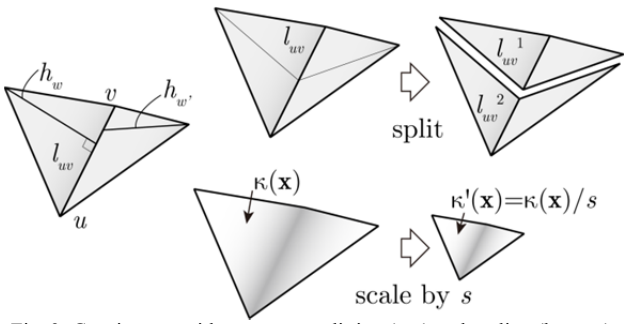

Fig. 3: Consistency with respect to splitting (top) and scaling (bottom).

3. CONSTRAINTS

By introducing additional geometric constraints for origami into this system, we can obtain design variations of bent origami form. We assume that the crease pattern is unchanged, i.e., the lengths of the edges (including triangulating edges) are preserved. Such a condition can be written as

$$\mathbf{L}(\mathbf{x}) = \{L_1 \ \cdots \ L_2\}^{\mathrm{T}} = \left\{\tfrac{1}{2}{l_1}^2 - \tfrac{1}{2}{l_1^0}^2 \ \cdots \tfrac{1}{2}{l_E}^2 - \tfrac{1}{2}{l_E^0}^2\right\}^{\mathrm{T}} = \mathbf{0}, \quad (10)$$

where l_i^0 is the target length of the edge i. Then, the overall constraints are represented as

$$[\mathbf{C_L}]\begin{Bmatrix}\delta\mathbf{x}\\ \delta\mathbf{w}\end{Bmatrix} = \begin{bmatrix}\frac{\partial \mathbf{F}}{\partial \mathbf{x}} & \frac{\partial \mathbf{F}}{\partial \mathbf{w}}\\ \frac{\partial \mathbf{L}}{\partial \mathbf{x}} & \mathbf{0}\end{bmatrix}\begin{Bmatrix}\delta\mathbf{x}\\ \delta\mathbf{w}\end{Bmatrix} = \mathbf{0}, \quad (11)$$

where the elements of Jacobean matrix $\frac{\partial \mathbf{F}}{\partial \mathbf{w}}$ and $\frac{\partial \mathbf{L}}{\partial \mathbf{x}}$ are,

$$\frac{\partial \mathbf{F}_u}{\partial w_i} = \frac{\partial \mathbf{A}_u}{\partial w_{vw}} = \begin{cases}\mathbf{x}_v - \mathbf{x}_u & \text{if } u = w\\ \mathbf{x}_w - \mathbf{x}_u & \text{if } u = v\\ \mathbf{0} & \text{else}\end{cases}, \quad (12)$$

$$\frac{\partial L_i}{\partial \mathbf{x}_u} = \frac{\partial L_{vw}}{\partial \mathbf{x}_u} = \begin{cases}(\mathbf{x}_v - \mathbf{x}_u)^{\mathrm{T}} & \text{if } u = w\\ (\mathbf{x}_w - \mathbf{x}_u)^{\mathrm{T}} & \text{if } u = v\\ \mathbf{0} & \text{else}\end{cases}. \quad (13)$$

Because the interior angle of each facet and the length and stiffness of each edge are constant, the elements of $\frac{\partial \mathbf{F}}{\partial \mathbf{x}}$ is written as

$$\frac{\partial \mathbf{F}_u}{\partial \mathbf{x}_v} = \sum_{\substack{\text{edge } i \text{ adjacent} \\ \text{or incident to } u}} \frac{\partial \mathbf{B}_u}{\partial \rho_i}\frac{\partial \rho_i}{\partial \mathbf{x}_v} + \sum_{\substack{\text{face } f \\ \text{incident to } u}} \frac{\partial \mathbf{B}_u}{\partial \mathbf{n}_f}\frac{\partial \mathbf{n}_f}{\partial \mathbf{x}_v} + \frac{\partial \mathbf{A}_u}{\partial \mathbf{x}_v}. \quad (14)$$

Here, by referring to equations (5), (6), and (7), $\frac{\partial \mathbf{B}_u}{\partial \rho_i}$ is represented as a linear combination of $\frac{k_i}{h_i}\cot\theta_{f,i,j}\,\mathbf{n}_f$, and $\frac{\partial \mathbf{B}_u}{\partial \mathbf{N}_f}$ as a linear combination of $\frac{k_i}{h_i}\rho_i \cot\theta_{f,i,j}$. The gradient $\frac{\partial \mathbf{n}_f}{\partial \mathbf{x}_v}$ of the normal vector of face f incident to v is a 3×3 matrix given by

$$\frac{\partial \mathbf{n}_f}{\partial \mathbf{x}_v} = [\mathbf{l} \quad \mathbf{m} \quad \mathbf{n}]\begin{bmatrix}0 & 0 & 0\\ 0 & 0 & -1/h_v\\ 0 & 0 & 0\end{bmatrix}\begin{bmatrix}\mathbf{l}^{\mathrm{T}}\\ \mathbf{m}^{\mathrm{T}}\\ \mathbf{n}^{\mathrm{T}}\end{bmatrix}, \quad (15) \quad (14)$$

where unit vectors $\mathbf{l}$, $\mathbf{m}$, and $\mathbf{n} = \mathbf{n}_f$ compose an orthogonal frame as shown in Fig.4. The last term in Equation (14) represents the force density method when force densities are constant.

$$\frac{\partial \mathbf{A}_u}{\partial \mathbf{x}_v} = \begin{cases}-\sum_{w \text{ incident } u} w_{uw} & \text{if } u = v\\ w_{uv} & \text{if } u \text{ is adjacent to } v.\\ \mathbf{0} & \text{else}\end{cases} \quad (16) \quad (14)$$

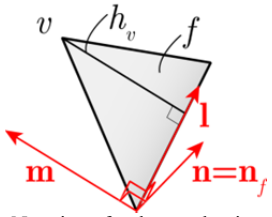

Fig. 4: Notation of orthogonal unit vectors.

4. SOLVING CONSTRAINTS

In a generic situation, Equations (8) and (10) yield an underdetermined system when multiple points are specified as pin supports. The number of degrees of freedom including 6 degrees of rigid motion is given by $3n_s$ where n_s is the number of support. This means that if we fix the positions of supporting vertices, we can obtain unique solution or discrete solutions. Therefore, straightforward method for obtaining a bending-active form is to minimize the bending energy while fixing the positions of the support arbitrarily. However, some set of support positions do no yield a valid bending form, and thus the design parameters cannot be arbitrarily set.

Our geometric approach naturally avoids this problem by directly solving the equilibrium conditions and assuming that the positions of the support are also variables. Therefore, the support configuration can be inversely calculated through 3D form finding. Equations (8) and (10) are satisfied in a state where each bending edge i satisfies $\rho_i = 0$ and no force is applied to each edge $\mathbf{w} = \mathbf{0}$. From such an initial solution, we can obtain a variety of forms through continuous variation satisfying Equation (11). We use an interactive approach by orthogonally projecting an estimate variation $\begin{Bmatrix}\delta\mathbf{x_0}\\ \delta\mathbf{w_0}\end{Bmatrix}$ specified by the user input to the linear subspace using Moore-Penrose generalized inverse $\mathbf{C_L}^+$ as,

$$\begin{Bmatrix}\delta\mathbf{x}\\ \delta\mathbf{w}\end{Bmatrix} = [\mathbf{I} - \mathbf{C_L}^+\mathbf{C_L}]\begin{Bmatrix}\delta\mathbf{x_0}\\ \delta\mathbf{w_0}\end{Bmatrix}, \quad (17)$$

similarly to solving kinematics of unstable transformable structures [3]. In the design system, the variation is discretized and numerically integrated. In order to eliminate the accumulated errors, generalized Newton-Raphson's method is applied. The generalized inverse solution for each step is calculated using the conjugate gradient method.

The initial estimate variation is indicated by dragging the vertices of the displayed structure through graphical user interface. Here, an interesting aspect is that the positions of structurally unpinned vertex can be directly modified, or even geometrically pinned to a given 3D position.

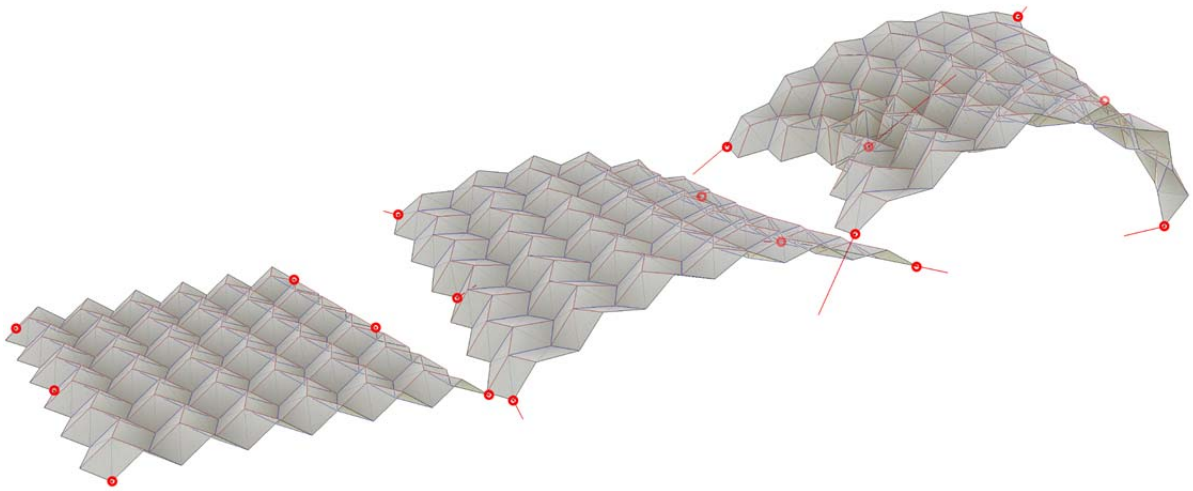

Fig. 5: Deformation of Miura-ori. Red circles and the segment from the circle indicate the support and the reaction force, respectively.

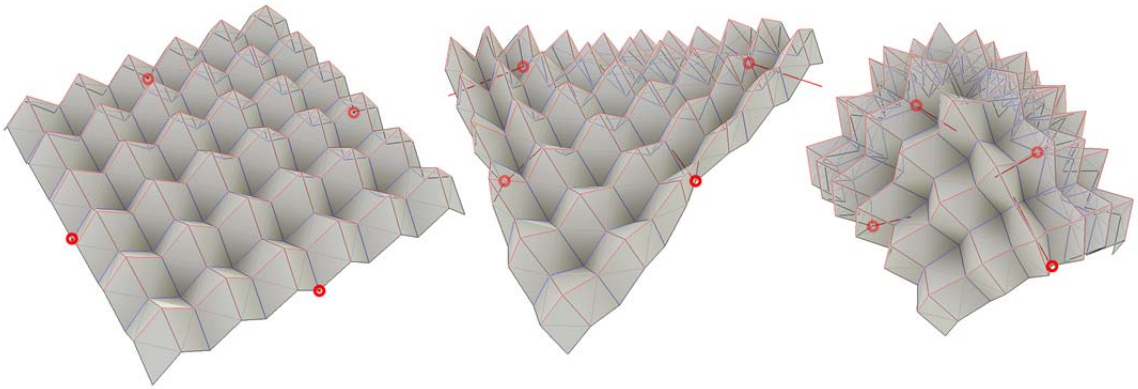

Fig. 6: Deformation of an eggbox sheet.

5. DESIGN EXAMPLES

5.1. Quad Mesh

We apply the design method to obtain form variations of quadrangle mesh origami. Miura-ori and Eggbox patterns are regarded as overconstrained one-DOF mechanisms when they are modeled as rigid origami, however when the bending behavior of each quadrangle is taken into account, their first eigenmodes can be globally anticlastic (Miura-ori) and synclastic (eggbox pattern) deformations as investigated by Shcenk and Guest [4].

Fig. 5 shows the form variations of Miura-ori in an equilibrium when 6 points on the boundary are set as the pin support of the structure. In total, the number of degrees of freedom is essentially determined by the support condition. With 6 pin supports, the structure forms a mechanism with 12 degrees of freedom (11 elastic + 1 rigid). Fig. 6 shows the form variations of eggbox pattern by varying the initial rigid origami state while the structure is supported at 4 points on the boundary, resulting in a mechanism with 6 degrees of freedom of transformation. Valid configurations include synclastic and anticlastic surfaces.

5.2. Kinematic Tessellated Surface

Since the positions of the support pins are inversely derived from the surface configuration, we can use our idea to the development of a kinematic surface system using thin elastic tessellated surface and small number of actuators. The concept is to use the design system to freely modify the 3D surface in the system while the surface configuration is interpreted as the positions of the support. A continuous transformation is thus recorded as the footprints or the paths of the supporting vertices, which can be used to control the physical tessellated origami model to form a freeform doubly curved surface. Fig. 7 Illustrates the concept of kinematic surface using the support pins as the controller.

5.3. Uncreased Surfaces

We can also approximate the bending of uncreased surfaces by appropriately meshing the surface along the rulings of the bent surfaces. Fig. 8 shows the calculated bending behavior of an elastic fan whose center point has a point crease. Fig. 9 represents a bent ribbon. This approximation qualitatively well captures the behavior of the bending of an uncreased continuous sheet. However, an uncreased developable sheet is a ruled surface whose ruling pattern can also continuously change. In order to truly capture this characteristic, a new method with the change in the mesh structure is necessary.

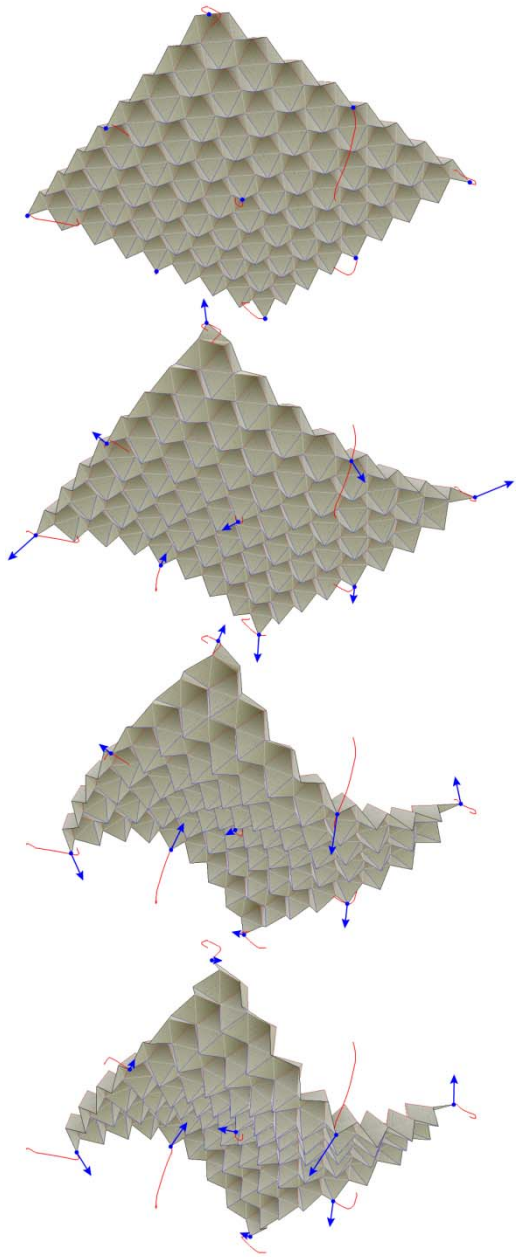

Fig. 7: Kinematic surface actuated by controlling the positions of 9 points (reaction force drawn in blue). The trajectory of the support is drawn in red.

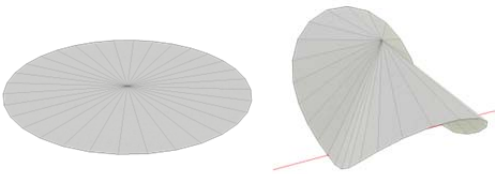

Fig. 8. Fan with a point crease in the middle.

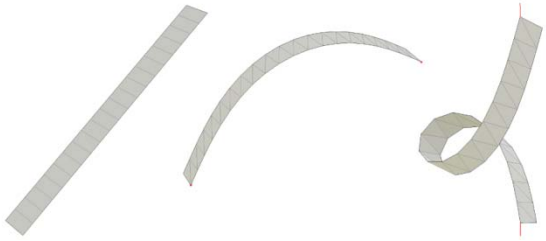

Fig. 9. Bending-active ribbon.

6. CONSIDERATION OF THE DIMENSION

In our method, the variation in the vertex coordinates $\delta\mathbf{x}$ and the force densities $\delta\mathbf{w}$ are packed in one vector variable. Since Equation (17) performs an orthogonal projection in the configuration space, the distance function in the configuration space can affect the result. For consistency, we describe $\mathbf{w}$ as in the length unit and thus k_{uv} in the cubed length. In order to avoid scale dependency, we use average length of the edge to normalize these parameters when we initialize the model. We can later scale the force densities proportionally; the scaling factor affects how the form responds to a given input deformation. The force densities can easily adapt to a given deformation when they are scaled smaller; as a relative result, the deformation is closer to the original user's input.

7. CONCLUSION AND FUTURE WORKS

We introduced a novel method to design origami forms governed by the bending of the panels by representing the configuration by the vertex coordinates and force densities, and then directly solving the equilibrium conditions as geometric constraints that form an underconstrained system. We introduced an interactive design system in which the user can intuitively find forms under equilibrium. Using the system, design variations of quadrangle panel origami tessellation models were achieved as well as an approximation of uncreased developable surface with bending. This leads to the idea of kinematic tessellated surfaces that can be controlled by actuating a small number of support vertices.

Our method assumes that the patterns do not change. Since the relocation of the rulings is essential in the bending of smooth developable surface, we would like to extend our method so that it allows for the change in the pattern. This is supposed lead to the simulation and design of curved folding structures. Another future work to be done is to treat the elastic stretch of the sheet as well as bending to capture different types of buckling of sheet material.

8. ACKNOWLEDGMENTS

This work was supported by JST, PESTO.

9. REFERENCES

[1] Tachi, T., *Geometric Considerations for the Design of Rigid Origami Structures*, in *Proceedings of IASS Symposium 2010*, Shanghai, China, (2010) pp. 771-782.

[2] Linkwitz, K., and Schek, H.-J. *Einige Bemerkungen zur Berechnung von vorgespannten Seilnetzkonstruktionen*, Ingeniuer-Archiv 40, 3, (1971) pp. 145–158.

[3] Hangai, Y., and Kawaguchi, K. 1991. Shape Analysis of Structures (Japanese: Keitai Kaiseki). Baifukan.

[4] Schenk, M., Guest, S.D., *Folded Textured Sheets*, In *proceedings of IASS 2009 Symposium*, September 28-October 2, 2009, Valencia, Spain (2009).